

# Evaluation of the suitability of various glass sealant—alloy combinations under SOFC stack conditions

V. A. C. HAANAPPEL\*<sup>‡</sup>, V. SHEMET<sup>‡</sup>, I. C. VINKE<sup>‡</sup>, S. M. GROSS<sup>§</sup>, TH. KOPPITZ<sup>§</sup>, N. H. MENZLER<sup>‡</sup>, M. ZAHID<sup>‡</sup>, W. J. QUADAKKERS

<sup>‡</sup>*Institute for Materials and Processes in Energy Systems and* <sup>§</sup>*Central Department of Technology, D-52425 Jülich, Germany*  
E-mail: v.haanappel@fz-juelich.de

The suitability of combinations of sealing material and alloy under simulated SOFC stack conditions has been evaluated by a novel test method. This method is based on test items of two metallic sheets, joined together with a glass or glass-ceramic sealant. The outer side of the sample is exposed to ambient atmosphere, whereas the inner side can be exposed to different gas compositions. The whole set-up is placed in a furnace. Optionally, an external voltage can be applied across the sheets.

Experiments revealed that the chemical and electrical behaviour of the sandwich samples strongly depends on the experimental conditions. Under oxidative conditions (air) no undesirable interactions take place, which detrimentally affect the electrical properties, indicating satisfactory suitability of the tested sealant—alloy combinations. However, different results were obtained when SOFC conditions were simulated by the use of a dual environment including air on the outer part and hydrogen on the inner part of the sample. Under these test conditions, and depending on the chemical composition of the alloy, a strong decrease of the resistance, measured between the two metallic sheets, was observed, due to excessive chemical reactions between the sealant, the alloy, and the surrounding gas atmosphere.

Well-chosen test conditions can more closely simulate real stack conditions, and as a result, the electrical, physical, and chemical behaviour of investigated samples is closer to that of materials applied in real SOFC stacks. Therefore, before performing model experiments simulating complete SOFC devices, it is recommended that a critical analysis should be made of the experimental conditions as present in SOFC devices.

© 2005 Springer Science + Business Media, Inc.

## 1. Introduction

Solid oxide fuel cells (SOFC) are promising energy devices for converting the chemical energy of fuel gases, such as hydrogen and methane, directly into electrical energy. Other advantages are that these SOFC devices in comparison to conventional energy production systems are clean, environmentally friendly due to low carbon dioxide emissions, and efficient. As a consequence, these devices are of major interest for stationary electricity and heat generation. Such a device, once it meets the targets for long-term durability and reliability, can compete with conventional energy conversion devices.

During the past decade Forschungszentrum Jülich (FZJ) has worked on advanced SOFC devices using planar cells and thin electrolytes. The design of these systems comprises planar stack designs with a large surface active area and flat anode substrate cells [1]. These de-

signs, indicated as type E-, F-, or G-design, are further adapted to obtain a satisfactory voltage output, which implies that the SOFCs are connected in serial mode using bipolar metallic interconnects. Glass-ceramic based materials from a BCAS (BaO-CaO-Al<sub>2</sub>O<sub>3</sub>-SiO<sub>2</sub>) system are often used for joining dissimilar materials, i.e. ceramic cells, metallic manifolds, and metallic interconnects [2–5]. These joints should be both gastight and electrically insulating, which implies that the sealants should separate (a) the fuel gas in the inlet and outlet channels from the oxidising environment, i.e. the cathode compartment and outer side of the stack (ambient atmosphere), and (b) the oxidising gas in the inlet and outlet channels from the anode compartment (fuel gas) and the outer ambient environment. In addition to these properties, the glass sealant should possess a satisfactory matching of the thermal expansion coefficient with

\* Author to whom all correspondence should be addressed.

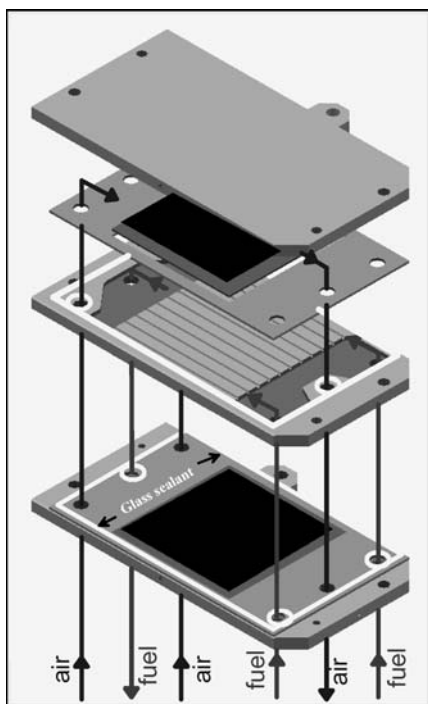


Figure 1 Schematic view of an E-design stack technology.

the cells and the chosen alloy, and it should also exhibit a long-term stability under oxidising as well as dual environmental conditions at high temperatures.

Fig. 1 shows a schematic view of a 2-cell stack in the so-called E-design with internal manifold and counter-flow configuration [1]. Fuel and oxidant gases both enter the stack from the bottom through two tubes, each arranged at the corners of opposite sides. In both layers, each containing one cell, the gases are distributed over the entire width of the cell inside the manifold. Through the channels in the interconnect the gases are distributed over the entire surface of anode and cathode. In the exit manifold the gases are collected in the centre and leave the stack via one tube on each side. In Fig. 1 the manifolds and gas channels on the fuel side are visible, although not all gas channels are drawn.

At present various stack components still suffer from degradation, which significantly limits the maximum operation time. This can partly be explained by chemical and physical interactions between the sealant and the alloy to be used for the interconnect and the manifold, and/or the surrounding gas atmosphere [2].

Several studies evaluating glass and glass-ceramic sealants are based on determining the chemical interactions between glasses and interconnect alloys [2, 6], characterisation of the crystallisation behaviour [3], or bond strength of a 'sandwich' sample during exposure in air at high temperatures [7]. The suitability of potential alloys to be used for the interconnect and/or manifold is generally based on oxidation experiments performed in either air, humidified hydrogen atmospheres, or carbon-containing fuel gases [8–12]. Other model studies, with respect to the development of construction materials for SOFC interconnects, are based on the improvement of a combination of properties required for the interconnect under real SOFC conditions [13–15].

Recent studies have shown that the presence of a dual atmosphere, i.e. hydrogen or steam on one side of the sample and air on the other, can have a significant effect on the oxidation behaviour of the underlying alloy [16–18]. In addition, and probably even more important, the interaction between the alloy and the sealant material depends on the type of oxide scale formed.

In this study the suitability of sealing material—alloy combinations under simulated conditions relevant for SOFC stacks will be evaluated by the introduction of a novel test method. With this method several experimental parameters affecting stack life can be varied systematically allowing a systematic approach to the influence of each parameter on the physical and chemical interactions between the sealant and the alloy.

## 2. Experimental

### 2.1. Experimental set-up

Experiments were performed with sandwich samples based on two metallic sheets, which were joined together by a glass paste applied by a dispenser. One of the sheets also contained a small hole allowing the desired gas composition to reach the inner part of the sample. In order to measure the electrical resistance of the joined couple, each sheet was connected to two Pt-wires, one to apply the desired external voltage over the glass sealant and the other to measure the current density. The samples were placed on top of a hermetically sealed alumina housing with four gas outlets. With this set-up a maximum of four samples could be tested simultaneously. A silver gasket was used to obtain sufficient gas tightness between the alumina housing and the sample.

After the sandwich samples were placed into the furnace, each sample was loaded by a weight of about 300 g. Joining of the metallic sheets and crystallisation of the glass sealant was carried out by a thermal cycle performed in air. The samples were heated to 850°C at 1°C/min. After reaching the temperature, a dwell time was set. This was followed by cooling the furnace down to 800°C at 1°C/min. During this temperature cycle organic solvents were removed, the glass was softened and a chemical interaction occurred between the glass sealant and the alloy resulting in sufficient bonding.

After the furnace reached the desired test temperature, in this case 800°C, the inner part of the alumina housing was flushed (100 ml/min ATP) with the desired gas composition: on the inner side hydrogen saturated with 3 vol% H<sub>2</sub>O, and on the outer part of the samples air. Optionally, an external voltage typically prevailing in SOFC stacks could be applied. All data were obtained by DC methods using a current-control power supply type Gossen 24K32R4 (Gossen-Metrawatt GmbH, Germany) and a computer-controlled data acquisition system including a datalogger type NetDAQ 2640A (Fluke, The Netherlands). Current density, external voltage, and consequently the electrical resistance were monitored continuously. If no external voltage was applied, the ohmic resistance was measured at regular intervals of approximately 24 h. A schematic set-up of the test unit is depicted in Fig. 2. After the total exposure

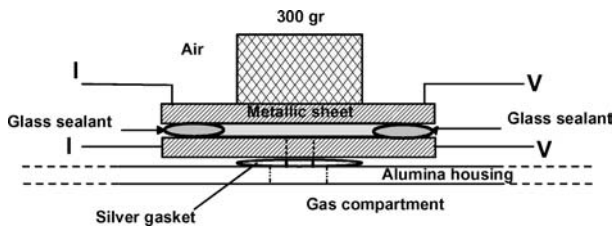


Figure 2 Schematic view of the experimental set-up for electrical resistance measurements during high temperature exposure in dual atmospheres.

time, the samples were cooled down to ambient temperature at a rate of  $1^{\circ}\text{C}/\text{min}$ . During cooling the inner part of the samples was flushed with argon.

With respect to the electrical behaviour of the samples as a function of the exposure time, plots are presented with the specific resistance on the *Y*-axis and the exposure time on the *X*-axis. The specific resistance is calculated from the measured ohmic resistance between the two metallic sheets and corrected for the total surface area and thickness of the glass sealant.

## 2.2. Material

Various series of experiments were performed with sandwich samples consisting of two metallic sheets of various types of model alloys including different surface treatments. Metallic sheets with a thickness of 2.0–3.0 mm were cut into  $50 \times 50$  mm squares, whereby one sheet contained a small hole in the centre (diameter: 10 mm). The surface of the alloy sheets was subsequently ground, polished, and ultrasonically cleaned with ethanol and acetone to remove organic substances. Table I shows the chemical composition of the various model alloys tested.

Two different glass sealants were used in this study, indicated as type A and B, the first was based on  $\text{Al}_2\text{O}_3$  (3.3 wt%),  $\text{SiO}_2$  (27.9 wt%),  $\text{CaO}$  (5.7 wt%),  $\text{BaO}$  (49.1 wt%), and the other on  $\text{Al}_2\text{O}_3$  (2.1 wt%),  $\text{SiO}_2$  (34.7 wt%),  $\text{CaO}$  (0.6 wt%),  $\text{BaO}$  (41.4 wt%). Both sealants include minor additions of transition metal oxides to optimise the SOFC relevant physical and chemical properties. The glass paste was applied by a disperser to the circumference of one sheet. An overview of the experiments with various alloy-glass sealant combinations under various experimental conditions is given in Table II.

TABLE I Chemical composition of the alloys used

Alloy	Fe	Cr	Mn	Ti	Si	Al	Re-el.	Ni
Alloy T-1	Bal.	22.6	0.4	0.06	0.1	0.1	La-0.1	0.2
Alloy T-2	Bal.	23.3	0.4	0.05	–	–	La-0.1	–
Alloy T-3	Bal.	22.1	0.5	–	0.4	0.2	Zr-0.1	0.3
Alloy T-4	Bal.	17.3	0.3	0.01	0.9	1.0	–	0.2
Alloy T-5	Bal.	22.1	0.4	0.05	0.1	–	La-0.1	–
Alloy T-6	Bal.	22.0	0.4	0.05	–	0.1	La-0.1	–
Alloy T-7	Bal.	22.7	0.4	0.04	–	–	La-0.05	–

## 2.3. Characterisation

Scanning electron microscopy (SEM) analyses of the surface morphology and cross sections was performed using a LEO 1530 electron microscope (Gemini).

## 3. Results

### 3.1. Electrical resistance measurements

The first series of electrical resistance measurements deals with purely oxidising conditions regarding various glass sealant—alloy combinations without (air–air, 0 mV) or with (air–air, 800 mV) an externally applied voltage. A second series is based on testing the sandwich samples in only hydrogen (3 vol% water vapour) without an externally applied voltage ( $\text{H}_2$ – $\text{H}_2$ , 0 mV). The third series deals with testing the sandwich samples in a dual atmosphere. This means that the inner part of the samples is exposed to hydrogen with 3 vol% water vapour and the outer part to ambient atmosphere. Also here, tests were performed without ( $\text{H}_2$ –air, 0 mV) and with ( $\text{H}_2$ –air, 800 mV) an externally applied voltage.

**Air–air, 0 mV:** Resistance measurements of a series of sandwich samples (nos. 1–18; see Table II) exposed in air–air at  $800^{\circ}\text{C}$  without an externally applied voltage showed no obvious degradation of the electrical resistance of the glass sealant. After 400 hrs of exposure the specific resistance of the samples was still more than  $1 \text{ k}\Omega\cdot\text{m}$ . This indicates that under these conditions no electrical shunt was formed between the two metallic sheets. In addition, no differences occurred between samples with either glass sealant type A or type B.

**Air–air, 800 mV:** In this case, only Alloys T-1 and T-2 were tested with glass sealant type A and B (sample nos. 19–22). In comparison with similar samples tested in air without an externally applied voltage, no obvious differences occurred between the electrical resistance as a function of the exposure time. The specific resistance was still high enough to avoid short circuiting.

**$\text{H}_2$ – $\text{H}_2$ , 0 mV:** The specific resistance of Alloy T-1 and T-2 with glass sealant type B (sample nos. 23 and 24) in only hydrogen with 3 vol% water vapour did not significantly change during 400 hrs of exposure at  $800^{\circ}\text{C}$ . The specific resistance over the whole exposure time was always higher than  $100 \Omega\cdot\text{m}$ . Fig. 3 shows the specific resistance of both alloy/glass combinations as a function of the exposure time.

**$\text{H}_2$ –air, 0 mV:** To investigate the effect of a dual gas atmosphere, one series of samples (nos. 25–26) was tested with air on the outer side and hydrogen (3 vol%  $\text{H}_2\text{O}$ ) on the inner side of the sample. In this case, no external voltage was applied. The specific resistance of the samples as a function of the exposure time is shown in Fig. 4. From this figure it is clear that in the case of Alloy T-1 after about 50 hrs of exposure the specific resistance was significantly reduced from almost  $10 \text{ k}\Omega\cdot\text{m}$  to less than  $1 \Omega\cdot\text{m}$ , whereas that for Alloy T-2 was always higher than  $10 \text{ k}\Omega\cdot\text{m}$  over the whole exposure time.

**$\text{H}_2$ –air, 800 mV:** Resistance measurements (with samples nos. 27–33) regarding Alloy T-1 and T-2 revealed that under a dual hydrogen—air atmosphere no obvious differences occurred between those tested

TABLE II Various alloy—glass sealant combinations regarding experiments performed at 800°C for 400 h under different experimental conditions

no.	Alloy	Glass sealant	Surface treatment	Gas comp. inner—outer side	Ext. appl. voltage (mV)
1	Alloy T-1	A	As-received	air - air	0
2	Alloy T-1	B	As-received	air - air	0
3	Alloy T-1	A	As-received + 100 hr/800 °C	air - air	0
4	Alloy T-1	B	As-received + 100 hr/800 °C	air - air	0
5	Alloy T-1	A	Polished + 100 hr/800 °C	air - air	0
6	Alloy T-1	B	Polished + 100 hr/800 °C	air - air	0
7	Alloy T-1	A	Hot-rolled, polished	air - air	0
8	Alloy T-1	B	Hot-rolled, polished	air - air	0
9	Alloy T-2	A	Polished	air - air	0
10	Alloy T-2	B	Polished	air - air	0
11	Alloy T-2	A	Polished + 100 hr/800 °C	air - air	0
12	Alloy T-2	B	Polished + 100 hr/800 °C	air - air	0
13	Alloy T-3	A	Polished	air - air	0
14	Alloy T-3	B	Polished	air - air	0
15	Alloy T-3	A	Polished + 100 hr/800 °C	air - air	0
16	Alloy T-3	B	Polished + 100 hr/800 °C	air - air	0
17	Alloy T-4	A	Polished + 100 hr/800 °C	air - air	0
18	Alloy T-4	B	Polished + 100 hr/800 °C	air - air	0
19	Alloy T-1	A	As-received	air - air	800
20	Alloy T-1	B	As-received	air - air	800
21	Alloy T-2	A	Polished	air - air	800
22	Alloy T-2	B	Polished	air - air	800
23	Alloy T-1	B	As-received	H <sub>2</sub> - H <sub>2</sub>	0
24	Alloy T-2	B	Polished	H <sub>2</sub> - H <sub>2</sub>	0
25	Alloy T-1	B	As-received	air - H <sub>2</sub>	0
26	Alloy T-2	B	Polished	air - H <sub>2</sub>	0
27	Alloy T-1	B	As-received	air - H <sub>2</sub>	800
28	Alloy T-2	B	Polished	air - H <sub>2</sub>	800
29	Alloy T-3	B	Polished	air - H <sub>2</sub>	800
30	Alloy T-4	B	Polished	air - H <sub>2</sub>	800
31	Alloy T-5	B	Polished	air - H <sub>2</sub>	800
32	Alloy T-6	B	Polished	air - H <sub>2</sub>	800
33	Alloy T-7	B	Polished	air - H <sub>2</sub>	800

without an externally applied voltage of 800 mV. Also here, after relatively short exposure times Alloy T-1 showed an obvious increase in conductivity. The specific resistance of Alloy T-2 was sufficiently high over the whole exposure time. Similar results were obtained with Alloy T-7. Fig. 5 shows the resistance as a function of the exposure time of Alloy T-1, T-2, and T-7 in a dual atmosphere at 800°C.

Additional measurements were made with Alloy T-1 to verifying reproducibility, Alloy T-5, and T-6 (see also Fig. 6). Here, it is clear that the use of Alloy T-1, T-3 and T-5 (see also Table I for the chemical composition of the tested alloys) adversely affected the electrical behaviour of the sandwich samples under the given experimental conditions. After about 250 h of exposure a substantial decrease of the resistance was observed. After about 70 h of exposure Alloy T-1 showed short circuiting, in a similar way as shown in Figs 4 and 5.

### 3.2. SEM analysis

Air-air: Fig. 7a shows the surface morphology of the inner part of a sandwich sample with Alloy T-1, exposed in air for 400 h at 800°C (no externally applied voltage). The outer surface of the alloy (top) consists mainly of a chromium- and manganese-rich oxide. Near the three-phase boundary, i.e. air-glass-alloy, a relatively high amount of a bright crystalline phase rich in barium, chromium, and oxygen was formed (Fig. 7b). Similar features were found with the other samples exposed in air. An external voltage of 800 mV did not obviously affect the reaction products formed near the three-phase boundary.

Cross-sectional analyses showed that the adhesion between the glass ceramic sealant and the alloy was always satisfactory. Figs 8a and b show micrographs of the cross section of Alloy T-2 with glass sealant type A. Here, different phases can be observed which are formed during the crystallisation cycle and probably

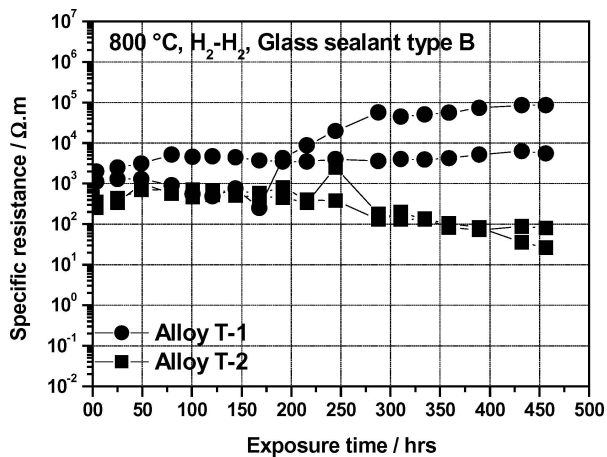


Figure 3 Specific resistance of Alloy T-1 and T-2 exposed in hydrogen at 800°C without an externally applied voltage.

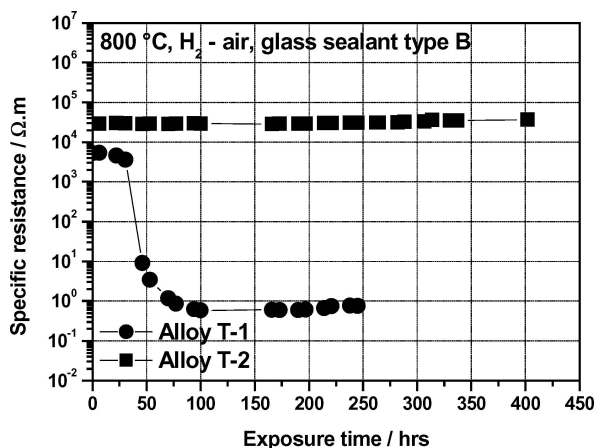


Figure 4 Specific resistance of Alloy T-1 and T-2 in a dual atmosphere at 800°C without an externally applied voltage.

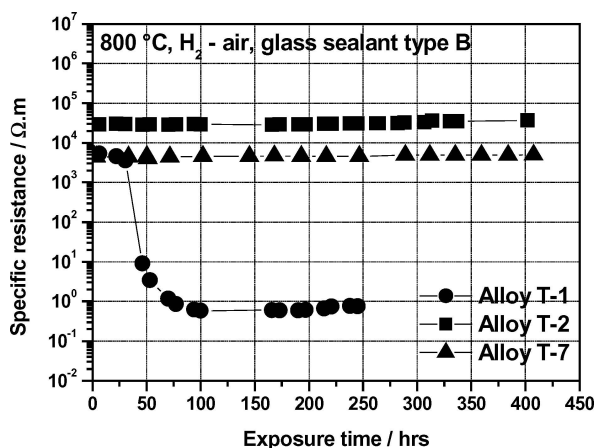


Figure 5 Specific resistance of Alloy T-1, T-2, T-7 in a dual atmosphere at 800°C with an externally applied voltage of 800 mV.

also during the long-term exposure at 800°C. Near the three-phase boundary (Fig. 8a) also a significant amount of a bright phase rich in Ba, Cr, and O, indicative of the formation of barium chromate was formed. No other oxidation products were found which might finally lead to degradation of the electrical resistance between the two metallic sheets.

Hydrogen–hydrogen: Two sets of sandwich samples, i.e. Alloy T-1 and Alloy T-2, both with glass sealant

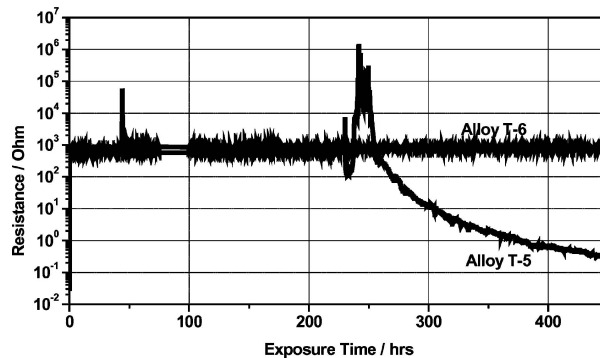
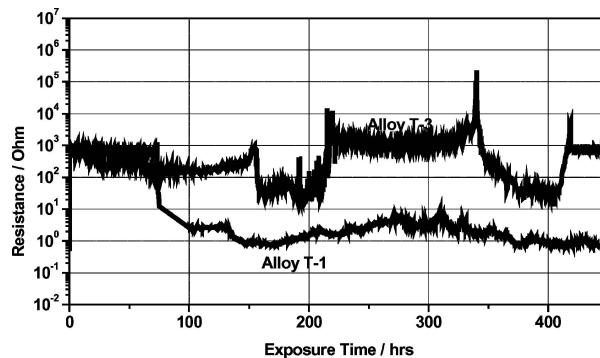


Figure 6 Specific resistance of Alloy T-1 and T-3 (upper part), and Alloy T-5 and T-6 (lower part) in a dual atmosphere at 800°C with an externally applied voltage of 800 mV.

type B, were also tested in hydrogen, saturated with 3 vol% H<sub>2</sub>O. During 400 h of exposure at 800°C no short-circuiting phenomena occurred, indicating that under these experimental conditions no highly conductive corrosion products were formed between the two metallic sheets. Removing the sheets from each other, it appeared that no yellowish reaction products (barium chromate), nor any brownish corrosion products (iron-containing oxides) were formed near the three-phase boundary.

Fig. 9 shows the surface morphology of Alloy T-1 with glass sealant type B near the three-phase boundary. The outer metallic surface shows the formation of only small oxide particles (bottom part of Fig. 9a). Interesting to note is the presence of small cracks parallel to the three-phase boundary. The glass sealant, as shown in Fig. 9a (upper part) and Fig. 9b, shows a crystalline structure, with crystals rich in Ba, Si, and O, or Ba, Ca, Si, and O. Cross-sectional analyses of the sandwich sample with Alloy T-1 (Fig. 10a) revealed severe internal oxidation of the alloy. This was not found in the case of Alloy T-2 (Fig. 10b). Here, a satisfactory adhesion between the glass sealant and the alloy can be observed.

Hydrogen–air: SEM analyses were performed on two positions of the inner surface area, i.e. at the air side and the hydrogen side. The morphology near the three-phase boundary at the hydrogen as well as at the air side of Alloy T-2 with glass sealant type B was comparable with that formed after 400 h of exposure at 800°C under purely oxidising conditions. Here, a dual atmosphere did not obviously change the formation of the various reaction products. In addition, the use of Alloy T-6 did not result in obvious detrimental effects either.

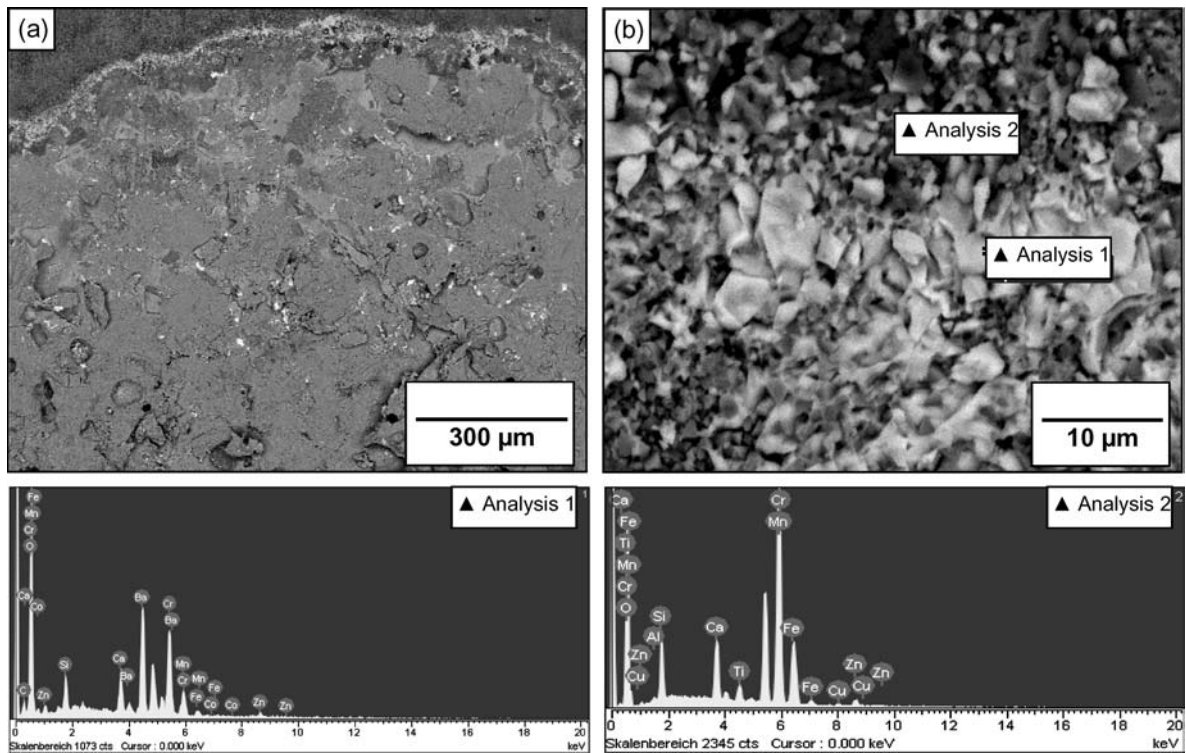


Figure 7 SEM micrographs of the surface morphology of Alloy T-1 with glass sealant type B after 400 h of exposure in air at 800°C. No external voltage was applied.

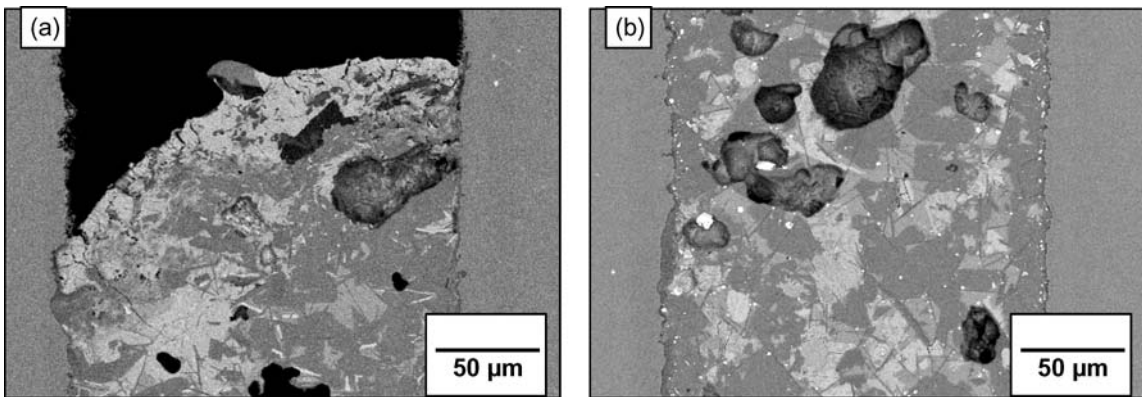


Figure 8 SEM micrographs of the cross section of Alloy T-2 with glass sealant type A after 400 h of exposure in air at 800°C. No external voltage was applied.

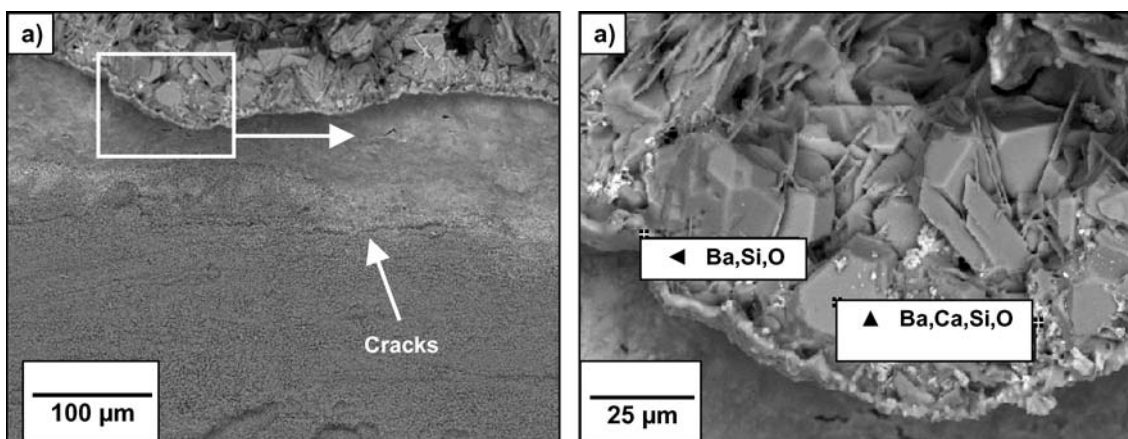


Figure 9 SEM micrographs of the surface morphology of Alloy T-1 with glass sealant type B after 400 h of exposure in hydrogen at 800°C. No external voltage was applied.

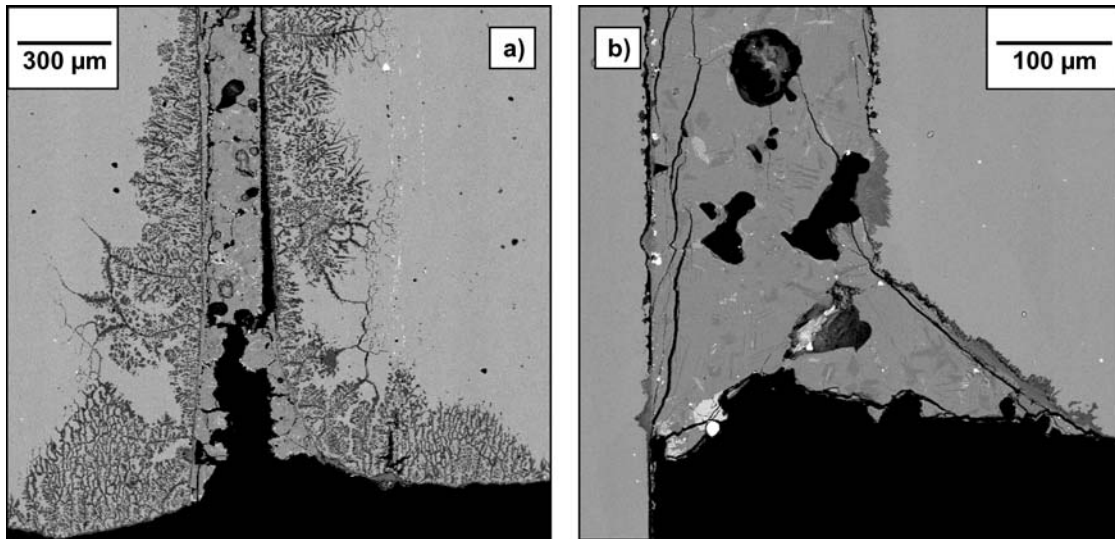


Figure 10 SEM micrographs of the cross section of Alloy T-1 (a) and Alloy T-2 (b) with glass sealant type B after 400 h of exposure in hydrogen at 800°C. No external voltage was applied.

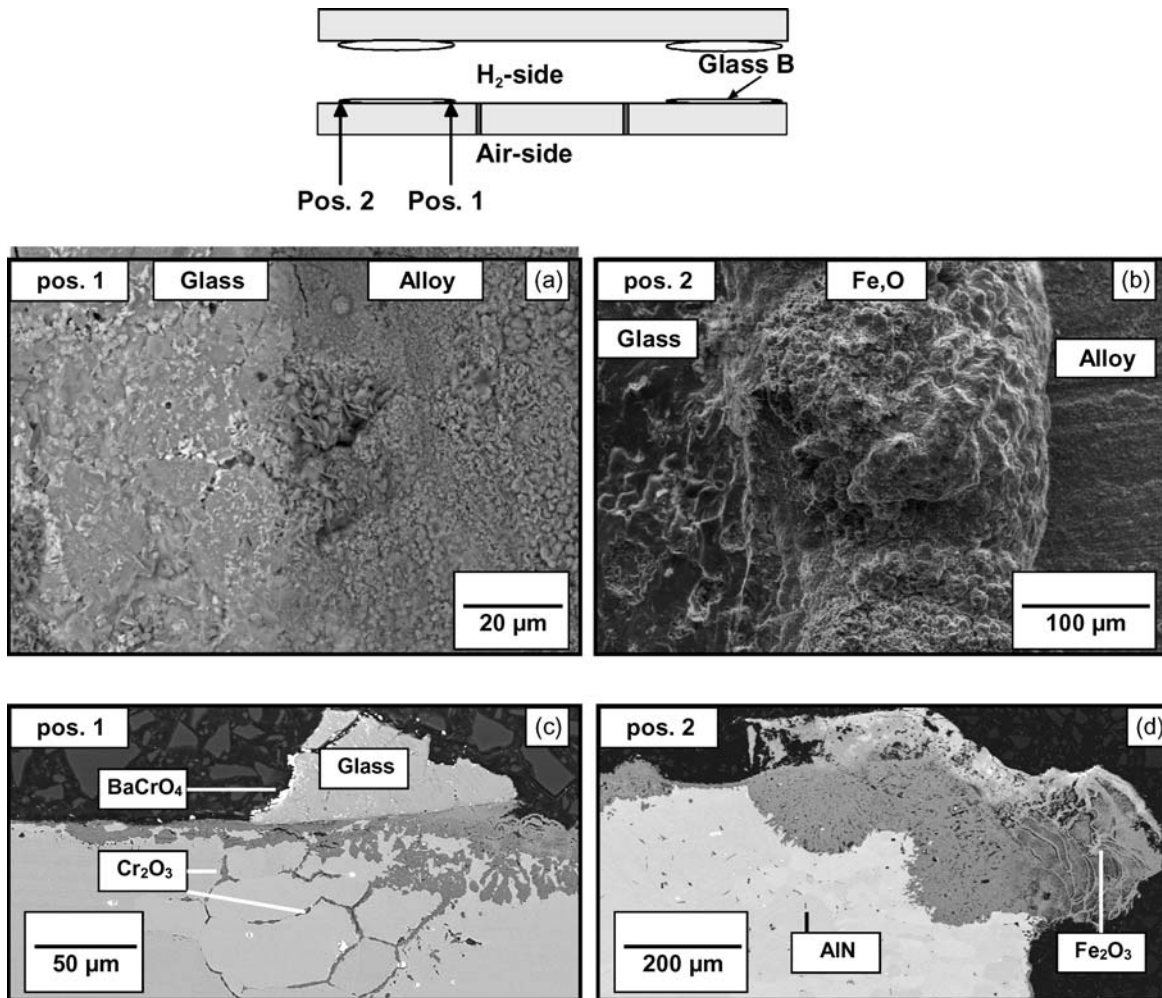


Figure 11 SEM micrographs of the surface morphology and cross sections of Alloy T-1 with glass sealant type B after 400 h of exposure in a dual atmosphere (hydrogen—air) at 800°C with an externally applied voltage of 800 mV.

With Alloy T-1 and glass sealant type B a different morphology was formed. Here, different reaction products were observed with respect to both three-phase boundaries. At the hydrogen side (see also Fig. 11a), the alloy surface near the glass sealant was covered with a fine-grained, thin oxide layer. No excessive oxide growth

was observed. On the air side and along the glass edge, large iron-containing oxide nodules were present. Excessive oxide growth occurred, which finally could lead to “bridge formation” between the two metallic sheets. Fig. 11b shows SEM micrographs of the surface morphology of Alloy T-1 with glass sealant type B after

400 h of exposure in a dual atmosphere at 800°C. In this case, an external voltage of 800 mV was applied. Furthermore, from SEM observations it was concluded that the presence of an external voltage of 800 mV did not obviously affect the formation of the various reaction products.

Figs 11c and d show the cross sections of the sample at both positions. Here, it is evident that on the hydrogen side only severe internal oxidation took place, whereas on the air side also external oxide growth occurred. Similar features were obtained with sandwich samples consisting of alloys T-3 and T-5 and glass sealant type B.

#### 4. Discussion

To obtain more insight into the relation between the chosen experimental parameters simulating SOFC stack conditions and the chemical and physical compatibility of glass sealants with various ferritic, chromia-forming alloys, different series of conductivity measurements (see Table II) were performed. The first series of measurements was based on samples, which were exposed in air for a period of up to 400 h. For a well-functioning SOFC stack, the formation of highly conductive oxide products between the manifolds and the interconnects has to be suppressed. Under the given conditions, these chosen test parameters specifically simulate that part of a stack, where the glass sealant insulates the cathode compartment (air) from the outer ambient atmospheric environment (see Fig. 1). Of course, glass sealants also have to fulfil other requirements, such as adapted viscosity, suitable thermal expansion coefficient, a wetting angle on the joining components of at least 90°, adapted flow and shrink behaviour, however, an in-depth discussion of these aspects is beyond the scope of this paper. Here, the discussion is limited to an evaluation of the introduction of a novel test method to analyse the suitability of sealing material—alloy combinations for SOFC stacks under various experimental conditions.

Conductivity measurements performed in air revealed no electrical degradation for any of the tested samples as listed in Table II. This means that during 400 h of exposure no highly conductive oxide products were formed which adversely affect the electrical insulation between the two metallic sheets. Furthermore, cross-sectional analyses revealed the formation of a yellowish reaction product, rich in Ba, Cr and O, along the edges of the glass sealant. The formation of this oxide can be explained by the presence of a chromium oxide scale which is in contact with the glass sealant containing BaO. Under oxidising conditions these species can form BaCrO<sub>4</sub>. At the interface between the glass sealant and the alloy, a thin chromium-rich oxide layer was formed. Here, no extensive formation of BaCrO<sub>4</sub> was found. Despite the formation of relatively large pores at the inner side of the glass sealant, as can be observed in Fig. 4, no cracks were found near the glass sealant—alloy interface. It can be suggested that the presence of these pores probably adversely affects the insulation capacity of the sealant, because they act as fast diffu-

sion paths for gaseous species. However, helium leak testing of these samples showed that the leakage rates were still within an acceptable range.

With the novel test method described in this paper, interaction between glass sealant and alloys can be critically evaluated. In this case the experimental conditions were closely related to those expected in real SOFC devices, i.e. separating cathode chamber and oxidant inlet and outlet channels from the outer ambient environment. From the observations, it was concluded that under purely oxidising conditions all listed glass sealant—alloy combinations showed satisfactory interaction. Moreover, type A and B are potential candidates to be used for stacks where the glasses have to separate the air in the channels and in the cathode compartment from the outer ambient environment due to the excellent compatibility of the glass sealant with the underlying alloy.

In order to investigate the effect of an external voltage on the interaction between the glass sealant and the adjacent alloy, the experimental set-up was slightly modified. Here, realistic stack operation conditions including a constant load were simulated, where the glass sealant separates the oxidant channels and the cathode chamber from the outer ambient atmosphere. In this case, two types of alloys, i.e. Alloy T-1 and Alloy T-2, were tested with glass sealant type A and B. Conductivity measurements as well as surface morphological and cross-sectional analyses of these samples showed that the results were similar to those observed under similar test conditions apart from an externally applied voltage. This means that with the above-mentioned alloy—sealant combinations the presence of an externally applied voltage of 800 mV is not required. However, care has to be taken in generalising these conclusions. It might be well possible that other alloy—sealant combinations have a higher dependence on the presence of an externally applied voltage.

The use of sandwich samples with hydrogen (humidified with 3 vol% H<sub>2</sub>O) at the inner side and air at the outer part of the sample simulates that part of a stack where the glass sealant has to reliably prevent mixing of the oxidising atmosphere with the fuel gas in the inlet and outlet channels and that in the anode chamber (see Fig. 1). Also, in this case, no differences occurred between samples exposed with or without an externally applied voltage. Noticeably different to the former observations, with samples exposed in only air, was the fact that under these experimental conditions including a dual atmosphere differences in the electrical and corrosion behaviour occurred. The ferritic steels T-1, T-3, and T-5 showed already a substantially decrease of the specific resistance after short exposure times, indicating the presence of an electrical shunt between the two metallic sheets. In the case of Alloys T-2 and T-6, the specific resistance was still quite high even after 400 h of exposure at 800°C in a dual atmosphere. Surface morphological and cross-sectional analyses showed that in the case of short circuiting significant amounts of voluminous corrosion products were formed, in addition to the formation of a Ba- and Cr-rich oxide. In particular, the formation of iron-rich



oxide products, often found near the three-phase boundary glass sealant—air—alloy, is worth noting. These fast growing and highly conductive oxides finally result in “bridge formation” between the two metallic sheets. In addition, severe internal oxidation of the alloy was observed. The iron-rich oxide products were not found near the three-phase boundary glass sealant—hydrogen—alloy. In this case, only internal oxidation of the alloy occurred.

These results show that with the given experimental conditions including a dual gas atmosphere of hydrogen and air, the electrical properties and corrosion behaviour of the sandwich samples strongly depends on the composition of the alloy and the glass sealant. Therefore, care has to be taken with respect to a thorough consideration of test parameters simulating the conditions prevailing in real SOFC stacks. Alloy—glass sealant combinations, which showed an excellent behaviour under purely oxidising conditions can still be very susceptible to internal and external oxide formation, the latter resulting in short-circuiting, under a dual atmosphere. Moreover, to create model studies simulating complete SOFC devices, which can be performed with this novel method, it is important to make a critical analysis of the experimental conditions as present in these SOFC devices.

For comparison reasons, tests were also made in only hydrogen with 3 vol% water vapour, however, without an externally applied voltage. In this case, only tests with Alloy T-1, T-2, and glass sealant type B were carried out. Conductivity measurements showed that the specific resistance of the two alloys was not obviously altered during 400 h of exposure at 800°C, indicating that no short circuiting had taken place. To investigate the interaction between the alloy and the glass sealant in more detail, surface morphological and cross sectional analyses were made. In the case of Alloy T-1, only internal oxidation was observed. This internal oxidation resulted in high internal stresses due to volume expansion, finally resulting in crack formation in the outer layer of the alloy. Another feature, which results from this effect is the reduced distance between the two metallic sheets. Initially, the distance between the sheets was about 200  $\mu\text{m}$ , however, it decreased to about 60  $\mu\text{m}$  after 400 h of exposure at 800°C. Therefore, it may well be possible that after longer exposure times the two sheets may come into contact with each other resulting in short circuiting. Besides, the two sheets can be pushed away from each other when excessive internal oxidation takes place at the glass sealant—alloy interface. These phenomena were only found for Alloy T-1 with glass sealant type B. In the case of Alloy T-2, no fast-growing external oxide products, nor internal oxidation or crack formation in the alloy near the three-phase boundary was observed.

## 5. Conclusions

- Significant differences occurred between the electrical properties and chemical behaviour of ‘sandwich’ samples when exposed in only ambient at-

mosphere or in a dual environment simulating SOFC stack conditions.

- Well carefully selected test conditions can simulate real SOFC stack conditions, and, as a result, the electrical, physical, and chemical behaviour of investigated samples are closer to that of materials applied in real SOFC stacks.
- Before performing model experiments to evaluate the behaviour of materials (combinations) in SOFC devices, it is recommended that a critical evaluation should be made of the experimental conditions prevailing in SOFC devices.

## Acknowledgements

The authors would like to thank the Central Department of Technology (Forschungszentrum Jülich GmbH, Germany), in particular Mr. A. Cramer for preparation of the sandwich samples. In addition, the authors gratefully acknowledge Dr. P. Batfalsky, Dr. D. Sebold, and Dr. E. Wessel for their assistance in SEM sample preparation and analyses, and Dr. F. Tietz, and the members of the TFK Group for their fruitful discussions.

## References

1. L. G. J. DE HAART, I. C. VINKE, A. JANKE, H. RINGEL and F. TIETZ, “New Developments in Stack Technology for Anode Substrate Based SOFC,” in Proceedings Solid Oxide Fuel Cells VII, edited by H. Yokokawa and S. C. Singhal (Electrochemical Society Proceedings, Pennington, USA,) (2001) Vol. 2001-16 p. 111.
2. Z. YANG, J. W. STEVENSON and K. D. MEINHARDT, *Solid State Ion.* **160** (2003) 213.
3. K. EICHLER, G. SOLOW, P. OTSCHIK and W. SCHAFFRATH, *J. Europ. Ceram. Soc.* **19** (1999) 1101.
4. S. B. SOHN, S. Y. CHOI, G. H. KIM, H. S. SONG and G. D. KIM, “Stable Sealing Glass for Planar Solid Oxide Fuel Cell,” *J. Non-Cryst. Solids* **297** (2002) 103.
5. T. SCHWICKERT, P. GEASEE, A. JANKE, U. DIEKMANN and R. CONRADT, “Electrically Insulating High-Temperature Joints for Ferritic Chromium Steel,” in Proc. Intern. Brazing and Soldering Conference, (Albuquerque, New Mexico, 2000) p. 116.
6. W. J. QUADAKKERS, J. PIRÓN ABELLÁN, V. SHEMET and L. SINGHEISER, *Mater. High Temperat.* **20**(2) (2003) 115.
7. J. PIRON-ABELLAN, V. SHEMET, F. TIETZ, A. GIL, L. SINGHEISER and W. J. QUADAKKERS, in Proceedings of Fifth European Solid Oxide Fuel Cell Forum, 1–5 July 2002, Lucerne/Switzerland, Vol. 1, p. 248.
8. K. L. LEY, M. KRUMPELT, R. KUMAR, J. H. MEISER and I. BLOOM, *J. Mater. Res.* **11**(6) (1996) 1489.
9. J. PIRON-ABELLAN, V. SHEMET, F. TIETZ, A. GIL, L. SINGHEISER and W. J. QUADAKKERS, SOFC-VII, June 3–8, 2001, EPOCHAL, Tsukuba, Japan, Proceedings of The Electrochemical Society, Pennington, NJ, USA, 2001, Vol. 2001-16, p. 811.
10. Z. YANG, K. S. WEIL, D. M. PAXTON and J. W. STEVENSON, “Selection and Evaluation of Heat-Resistant Alloys for SOFC Interconnect Applications,” *J. Electrochem. Soci.* **150**(9) (2003) A1188.
11. T. SCHWICKERT, P. GEASEE, I. KREUTZER, U. REISGEN and R. CONRADT, “Characterization of the Bonding Strength of Glass Ceramic Steel Joints,” in Proceedings of the “5th European Solid Oxide Fuel Cell Forum,” edited by J. Huijsmans, The European Fuel Cell Forum, (Switzerland) (2002) p. 319.
12. T. J. ARMSTRONG, M. A. HOMEL and A. V. VIRKAR, “Evaluation of Metallic Interconnects for Use in Intermediate Temperature SOFC,” in Proceedings of the International Symposium “Solid Oxide Fuel Cells VIII,” edited by S. C. Singhal and

- M. Dokiya (The Electrochemical Society, 2002) Vol. 2003-07, p. 841.
13. T. HORITA, Y. XIONG, K. YAMAJI, N. SAKAI and H. YOKOKAWA, *J. Electrochem. Soc.* **150**(3) (2003) A243.
  14. P. FRIEHLING and S. LINDEROTH, "Evaluation of Ferrite Stainless Steels as Interconnects in SOFC Stacks," in Proceedings of the "5th European Solid Oxide Fuel Cell Forum," edited by J. Huijsmans, The European Fuel Cell Forum, Switzerland 2002, p. 855.
  15. L. JIAN, J. HUEZO and D. G. IVEY, *J. Power Sourc.* **123** (2003) 151.
  16. K. HUANG, P. Y. HOU and J. B. GOODENOUGH, *Solid State Ionics* **129** (2000) 237–250.
  17. Z. YANG, M. WALKER, G. XIA, P. SINGH and J. W. STEVENSON, *Electrochem. Solid-State Lett.* **6**(10) (2003) B35.
  18. K. NAKAGAWA, Y. MATSUNAGA and T. YANAGISAWA, *Mater. High Temperat.* **18**(1) (2001) 51.

*Received 8 June  
and accepted 8 November 2004*